Available online at www.sciencedirect.com
ScienceDirect
LITHOS
Lithos 97 (2007) 174 – 192
www.elsevier.com/locate/lithos

Cretaceous Gross Spitzkoppe and Klein Spitzkoppe stocks in Namibia: Topaz-bearing A-type granites related to continental rifting and mantle plume

I. Haapala [a,*], S. Frindt [b], J. Kandara [c]

[a] Department of Geology, P.O. Box 64, FI-00014 University of Helsinki, Finland
[b] Geological Survey of Namibia, P.O. Box 2168, 1 Aviation Road, Windhoek, Namibia
[c] Rosh Pinab Zinc Corporation (Pty) Ltd, P.O. Box 115, Rosh Pinab, Namibia

Received 3 February 2006; accepted 4 December 2006
Available online 26 January 2007

Abstract

The anorogenic Damaraland intrusive complexes in Namibia belong to the bimodal Paraná–Etendeka Large Igneous Province and comprise mafic, silicic and alkaline plutonic and volcanic rocks that were emplaced into the Neoproterozoic Damara orogenic belt at 124 to 137 Ma. The magmatism was related to the Tristan mantle plume and continental rifting that led to separation of South America from Africa. Silicic plutonic rocks are found in the Gross Spitzkoppe, Klein Spitzkoppe, Erongo, Brandberg, Messum, Cape Cross, and Paresis complexes. The Gross Spitzkoppe and Klein Spitzkoppe stocks consist of texturally distinct types of topaz-bearing biotite (siderophyllite–annite) granites with columbite, zircon, magnetite, and monazite as typical heavy accessory minerals. A bimodal magmatic association is indicated by synplutonic mafic dikes and magmatic mafic inclusions. The stocks have rims of layered aplite–pegmatite stockscheiders against the country rocks. Miarolitic cavities and pegmatite-lined druses with gem-quality topaz and beryl indicate vapor saturation, and hydrothermal activity has locally produced wolframite-bearing greisen. The Spitzkoppe granites are highly evolved, marginally peraluminous (A/CNK 0.95 to 1.09) and characterized by high SiO_2 (74.4 to 78.6 wt.%), Na_2O+K_2O (7.6 to 8.8 wt.%, with K_2O prevailing over Na_2O), F, Rb, and Ga, as well as low MgO, Ba, and Sr. The small but clear differences in REE patterns [$(La/Yb)_N$ in Gross Spitzkoppe 2.5 to 7.7 with mean at 4.4, in Klein Spitzkoppe 0.6 to 1.6 with mean at 0.9, more pronounced negative $(Eu/Eu^*)_N$ anomaly in Klein Spitzkoppe] show that the granites of the Klein Spitzkoppe stock are slightly more evolved than those of the Gross Spitzkoppe stock. Overall, the granites exhibit A-type and within plate characteristics.

Available O, Nd and Sr isotope data suggest that the silicic rocks of the anorogenic Damaraland complexes have mixed sources, with plume-related mantle magmas and two types of lower crustal sources (orogenic Damara basement and pre-Damara gneisses) as end members. The mantle component prevails in the metaluminous and peralkaline granites of the Brandberg complex, whereas Damara crustal rocks were dominant in the source of the cordierite-bearing peraluminous granodiorites and tourmaline-bearing granites of the Erongo complex. Pre-Damara gneisses are the main source component in the Paresis rhyolites. The Spitzkoppe and Cape Cross granites have both major mantle and crustal (Damara) sources. Although it is not possible to identify a unique

* Corresponding author. Tel.: +358 9 590400; fax: +358 9 19150826.
E-mail address: ilmari.haapala@helsinki.fi (I. Haapala).

doi:10.1016/j.lithos.2006.12.002

petrogenetic process by which the Damaraland complexes formed, it is clear that the magmas formed in an extensional environment and that both mantle and crustal sources were involved in production of these magmas.

Keywords: A-type granite; Rifting; Mantle plume; Petrogenesis; Geochemistry

1. Introduction

The Paraná (Brazil)–Etendeka (Namibia) flood volcanic and associated plutonic rocks represent one of the Large Igneous Provinces (LIP) of the Earth. This umbrella term, introduced by Coffin and Eldholm (1994), includes continental flood basalt–rhyolite (*sensu lato*) provinces, oceanic plateaus, volcanic rifted margins, and aseismic ridges that represent anomalously high magmatic fluxes. The Paraná–Etendeka igneous province is bimodal (basaltic–rhyolitic) and was formed about 130 Ma ago in connection with the onset of upwelling of the Tristan mantle plume and break-up of the western Gondwana supercontinent, which led to the opening of the Atlantic Ocean (White and McKenzie, 1989). This continental rifting developed into seafloor spreading at about 125–127 Ma, as indicated by the oldest linear magnetic anomalies (E4) off the coast of Namibia (Gladczenko et al., 1997). The track of the hot-spot volcanism can be followed on the African side along the Walwis Ridge from the Etendeka area to the Tristan da Cunha volcanic island group; on the South American side the track is represented by the Rio Grande Rise (Fig. 1; White and McKenzie, 1989; O'Connor and Duncan, 1990). The plume head was situated below the Paraná–Etendeka igneous province and may have been more than 2000 km in diameter.

Although the Paraná–Etendeka province is known principally as a volcanic province, it includes also a number of subvolcanic and plutonic complexes, which in most cases show evidence for bimodal magmatism. Several complexes contain granitic plutons and thus

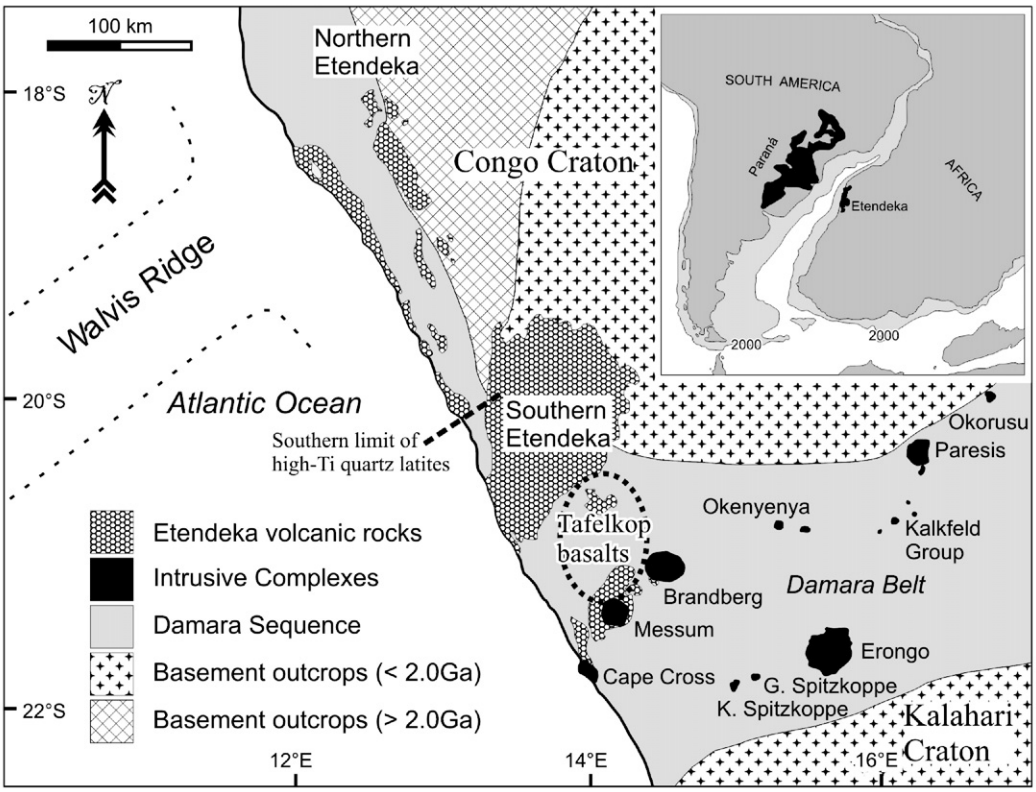

Fig. 1. Main geological features of northwestern Namibia (Milner et al., 1995; le Roex and Lanyon, 1998) showing the Cretaceous Etendeka Group volcanic rocks and the Damaraland intrusive complexes. The index map shows the Paraná–Etendeka province soon after the separation of Africa and South America (White and McKenzie, 1989).

yield a unique possibility to study granitic magmatism in all probability related to continental rifting and mantle plume activity. Our studies of the Gross Spitzkoppe and Klein Spitzkoppe granite stocks were started in 1994 and the results have been presented as unpublished academic theses (Frindt, 1997; Kandara, 1998) and several petrological–geochemical articles (Frindt and Poutiainen, 2002; Frindt and Haapala, 2002; Frindt et al., 2004a,b; Frindt and Haapala, 2004; Haapala et al., 2005). This paper is a review based on these and other studies (e.g., Pirajno, 1990; Harris, 1995; Schmitt et al., 2000; Mingram et al., 2000; Trumbull et al., 2000, 2003; Bauer et al., 2003; Trumbull et al., 2004) on the Damaraland igneous complexes.

2. The Etendeka volcanic rocks

The Tertiary Paraná–Etendeka volcanic association is strictly bimodal and mainly comprises continental flood basalt and, in the upper parts of the volcanic series, voluminous rhyolitic (*sensu lato*) interbeds (quartz latite or rhyodacite, rhyolite, trachyte). Silicic volcanic rocks are much more abundant (about half of the total thickness of the volcanic series) in the Etendeka area than in Paraná (about 3%), which is explained by the asymmetry of the Paraná–Etendeka province relative to the Atlantic rift, and the fact that the silicic volcanites are especially associated with the rift (Ewart et al., 2004a). Otherwise, the lavas, dikes, and sills show similar petrographic and geochemical characteristics on both sides of the Atlantic (Marsh et al., 2001; Ewart et al., 2004a,b).

The mafic series (e.g., the Tafelberg and Khumib basaltic series) include members from basalt to trachyandesite, in the northern Etendeka also some latitic interbeds are found (Ewart et al., 2004b).

The mafic lavas vary from tholeiitic to alkaline. Geochemical differences exist especially in the contents of the high field strength elements (HFSE). The mafic lavas have been divided into high-Ti and low-Ti types and a corresponding characterization can be expanded to the silicic volcanic rocks (e.g., Ewart et al., 2004a,b; Garland et al., 1995). In the Etendeka volcanic field, the distinction between high-Ti and low-Ti basaltic series is based on the TiO_2 and Sr contents, the lower limit of high-Ti series is at 2.2 wt.% TiO_2 and 450 ppm Sr (Marsh et al., 2001; Ewart et al., 2004a). High-Ti lavas (Khumib type) occur only in the northernmost Etendeka field (Fig. 1), and most of the mafic lavas and dikes are of the low-Ti type. The Tafelkop lavas north of the Messum complex (Fig. 1) as well as the Messum basanite dikes (Harris et al., 1999) and ferro-picritic dikes and associated lavas (Thompson et al., 2001) exhibit isotopic compositions that correspond to those of the Tristan plume basalts ($\varepsilon_{Nd} \sim 0$ to $+7$, initial $^{87}Sr/^{86}Sr$ around 0.705). This suggests that these lavas and related rocks are plume derived. Most of the Etendeka mafic and silicic lavas have, however, negative ε_{Nd} values (-3 to -12) and varying initial $^{87}Sr/^{86}Sr$ values (0.707 to 0.721; Ewart et al., 1998a,b, 2004a,b), which may be, directly or indirectly, related to crustal source components, as will be discussed in Section 5.1.

3. The Damaraland intrusive complexes — an overview

The Damaraland intrusive complexes comprise at least 20 subvolcanic–epizonal intrusions within the E-trending Neoproterozoic Damara orogenic belt between the Kalahari craton in the south and the Congo craton in the north (Fig. 1). The complexes extend in two NE-trending zones from the coast (Cape Cross) about 350 km inland (Okorusu). Based on the principal rock associations, they can be grouped into granitic (Brandberg, Erongo, Gross and Klein Spitzkoppe, Cape Cross, Paresis), differentiated mafic (Messum, Okenyena, Cape Cross), and carbonatite–alkaline rock complexes (e.g., the Kalkfeld group, Okorusu). The granitic complexes are situated in the western part of the belt, the carbonatite–alkaline rock complexes farther in the east. The ages of the plutons vary from 124 to 137 Ma (Milner et al., 1995). The youngest ages, about 125 Ma, are obtained for the Gross Spitzkoppe granite as well as alkaline rocks and lamprophyre dikes of the Okenyena and Okorusu complexes (Frindt et al., 2004b; Milner et al., 1995; le Roex and Lanyon, 1998). In the following, the main petrological features of the silicic complexes of Erongo, Brandberg, Messum, Cape Cross and Paresis are briefly summarized. The Gross and Klein Spitzkoppe stocks are described in more detail in Section 4.

The caldera-like *Erongo volcanic–plutonic complex* (Pirajno, 1990) has a diameter of about 35 km and consists of basal basaltic lavas and a 1 km thick series of rhyodacitic–rhyolitic ash-flow tuffs, intruded by a central peraluminous, cordierite-bearing granodiorite and tourmaline-bearing biotite granite (Erongo granite) as well as minor alkaline plugs. A semi-circular diabase ring dike surrounds the complex. The Erongo granite is found as isolated stocks and irregular plutons along the caldera-type structure. The main granite is prevailingly even-grained with an average mode of 36% quartz, 33% K-feldspar, 25% albite, 4.5% biotite, and 1.5% accessory minerals (tourmaline, fluorite, topaz, zircon, apatite), but has a porphyritic roof facies (Pirajno, 1990). Tourmaline is found (1) as an accessory mineral in the granite matrix, (2) in quartz–tourmaline nests, up to 30 cm in diameter, in the granite replacing feldspars and biotite, (3) in miarolitic cavities and pegmatite pockets together with gem-quality beryl and topaz, and (4) as fracture-controlled veinlets in the granite.

The Brandberg granite complex (Schmitt et al., 2000) is about 25 km in diameter. It mainly consists of an even-grained metaluminous hornblende–biotite granite that intrudes an earlier pyroxene–hornblende monzonite and is intruded by leucocratic biotite granite dikes. At the southeastern margin, the main granite is intruded by volumetrically minor peralkaline arfvedsonite granites of the Amis complex.

The *Messum ring complex* is about 18 km in diameter and consists of a diverse assemblage of alkaline and tholeiitic intrusive and extrusive rocks. Although the complex intrudes the volcanic sequence of the Gobobeseb Mountains (Etendeka Province), its plutonic rocks show isotopic ages similar to the Etendeka lavas (gabbros and diorites 131.7 ± 0.7 Ma to 132.1 ± 1.2 Ma, nepheline syenite 129.3 ± 0.7 Ma, Etendeka lavas 131.9 ± 0.6 Ma to 132.9 ± 1.2 Ma; Renne et al., 1996). The Messum complex has an outer zone of gabbroic cone sheets interleaved with anorthosite and granitoids, a poorly exposed intermediate zone containing quartz syenitic and granitic intrusions, and a heterogeneous core zone with nepheline syenite and quartz syenite intrusions and breccias (Harris et al., 1999; Bauer et al., 2003). Integrated reflection and refraction seismic soundings, gravity and aeromagnetic data indicate that the ring complex continues down to the Moho depths (40 km) as a cylindrical high velocity and high density zone with roughly the same cross sectional area as on the surface (Bauer et al., 2003). This zone is modeled as a network of mafic intrusions with about 30% gabbroic rocks, and the overall amount of intruded mafic material increases at depth. The relative amount of felsic material seems to increase upward, suggesting that some magmatic evolution took place during the ascent. Bauer et al. (2003) concluded that the magma transport and emplacement along the heavily intruded root zone took place in brittle fraction at all levels of the crust, and were controlled by conditions of high fluid (magma) pressure and high magma flux.

The Cape Cross ring complex is poorly exposed and lies partly offshore. It contains granophyric microgranite, nepheline syenite, and gabbro (Trumbull et al., 2004). Gravity, aeromagnetic and seismic P-velocity anomalies suggest that the complex has a similar cylindrical intrusive zone through the crust as the Messum complex (Bauer et al., 2003). The 137 Ma *Paresis volcanic–subvolcanic complex* (Mingram et al., 2000)

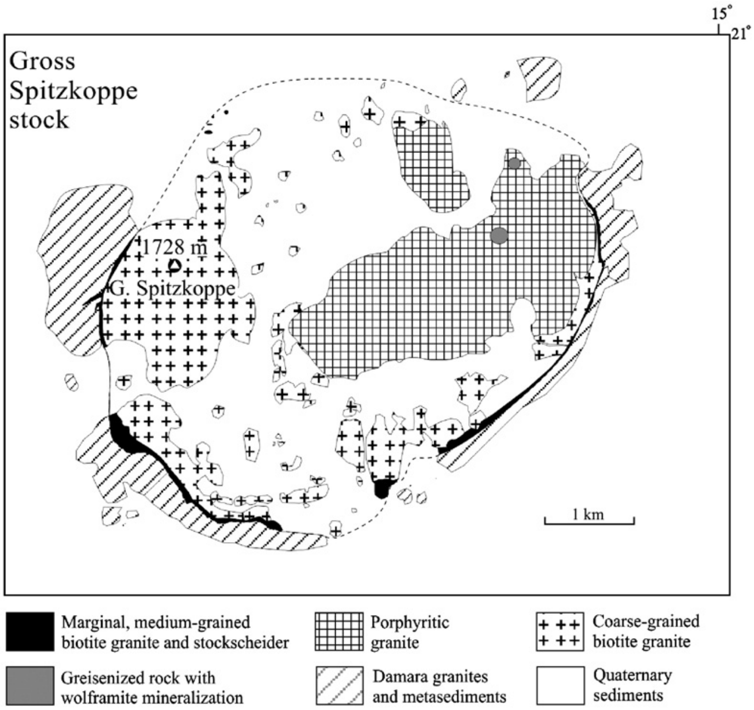

Fig. 2. Geological map of the Gross Spitzkoppe granite stock, simplified from Frindt et al. (2004a).

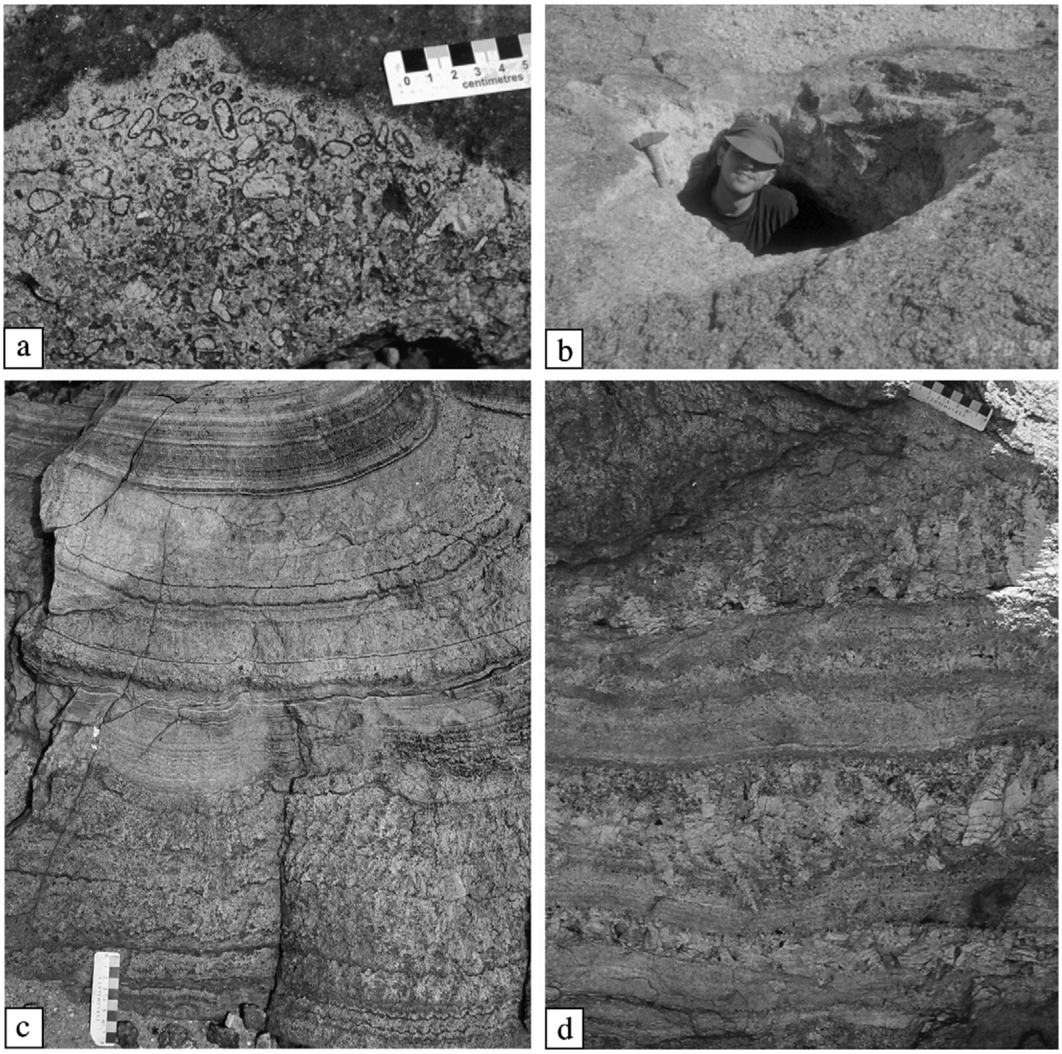

Fig. 3. Structural and textural features in the Gross Spitzkoppe and Klein Spitzkoppe granite stocks. (a) Mingling and hybridization textures between porphyritic granite and mafic enclaves (upper margin of the picture) at the northeastern margin of the Gross Spitzkoppe stock. The alkali feldspar phenocrysts are corroded and mantled by plagioclase shells. (b) Large miarolitic cavity in porphyritic granite, Gross Spitzkoppe stock. Such druses contain gem-quality topaz and beryl crystals. (c) Layered aplite stockscheider at the margin of the Gross Spitzkoppe stock. Growth direction downward (see Frindt and Haapala, 2004). (d) Layered pegmatite stockscheider dike at southeastern margin of the Klein Spitzkoppe stock.

measures 18 km by 16 km in plan. The exposed rocks are dominated by rhyolitic flows with some comendites and basaltic lavas. The subvolcanic rocks are mainly microgranites, syenites, nepheline syenites, and other feldspathoid-bearing rocks and gabbros. Lamprophyre dikes cut the other rocks of the complex.

4. The Spitzkoppe topaz granite stocks

4.1. The Gross Spitzkoppe stock

The Gross Spitzkoppe stock is an impressive 30 km^2 inselberg and landmark of the area, rising about 700 m above the flat ground level (Fig. 2). Country rocks include Damara mica schists and gneisses with carbonate rock and skarn intercalations as well as Damara S-type granites and tourmaline-rich pegmatites. The stock consists of various textural types of topaz-bearing granite, and a bimodal character of the magmatism is indicated by synplutonic mafic dikes and locally abundant magmatic mafic enclaves. Occasionally, the hybridized granite may contain also corroded and plagioclase-mantled alkali feldspar megacrysts (Fig. 3a; see also Frindt et al., 2004a). Subhorizontal and steeply dipping microgranite dikes and two lamprophyre dikes cut the main granites (Frindt et al., 2004a,b) and the

Table 1
Average modal compositions and other petrographic characteristics of the main granite types of the Gross Spitzkoppe and Klein Spitzkoppe stocks

	Gross Spitzkoppe			Klein Spitzkoppe	
	Marginal granite	Coarse-grained granite	Porphyritic granite	Coarse-grained granite	Medium-grained granite
Texture	Equigranul. (-porphyrit.)	Equigranul.-seriate	Porphyritic	Seriate	Equigranul. -porphyritic
Grain size mm Megacrysts	2–5 (K-feldspar, quartz)	10–20	1–5 K-feldspar, quartz	2–8	1–5 K-feldspar, quartz
Quartz	31.1 e, s–a	37.8 e–a	36.4 e–s, a	36.3 e, s–a	35 e, s–a
K-feldspar	40.4 s–a	37.6 s, a	30.4 s–e, a	41.6 s, a	44 s, a
Plagioclase	20.2 e, s	16.4 e–s	24.6 e–s	17.0 e–s	17 e–s
Biotite (in part altered)	7.8 s, a	6.4 s, a	4.0 s	3.5 a–s	2 a–s
Topaz	0.1 s, a	1.3 s, a	2.7 s, a	0.9 s, a	1 e–s, a
Fluorite	0.8 s, a	p s, a	1.4 s, a	1.0	1 s
Accessory heavy minerals*	0.2	0.4	0.4	p	p

e, euhedral; s, subhedral; a, anhedral; p, present in small amounts or erratically.
* In Gross Spitzkoppe granites zircon, columbite, magnetite, monazite, thorite, apatite, ilmenite, rutile, and allanite (in coarse-grained granite), in Klein Spitzkoppe granites zircon, columbite, monazite, and magnetite.

stock is rimmed by a layered aplite–pegmatite stockscheider which shows unidirectional solidification textures (UST) (Fig. 3c; Frindt and Haapala, 2004).

The stock consists of four textural types of topaz-bearing biotite granite (Table 1).

(1) Marginal medium-grained equigranular or weakly porphyritic granite that forms an up to 150 m wide outer zone of the stock. The granite is characterized by the presence of small globules or globule swarms of magmatic mafic enclaves. Locally the granite is in direct contact with the Damara country rocks, but typically the stock contact is marked by the aplite–pegmatite stockscheider.

(2) Coarse-grained granite is the prevailing granite type of the stock. It has in places sharp sinuous contacts with the marginal granite; in places the contact is gradational. Various structural types (linear, circular, elliptic, horse tail, ladder dike) of biotite-rich schlieren are found in this granite, demonstrating movements and fractionation in the crystallizing magma chamber (Frindt et al., 2004a).

(3) Porphyritic granite is found in the central and eastern part of the stock. The fine- to medium-grained groundmass contains K-feldspar and quartz megacrysts. Miarolitic cavities are common, indicating crystallization from fluid-saturated magma (Fig. 3b).

(4) In the eastern part of the stock, a small cupola of porphyritic microgranite intrudes the pophyritic granite. The contact is marked by a 1 m thick aplitic or pegmatitic stockscheider that contains plumose K-feldspar crystals flaring towards the center of the cupola. The grain size of the matrix changes from fine-grained near the margins to medium-grained in the central parts of the cupola. Topaz is present as up to 2.5 mm long subhedral crystals and as anhedral interstitial grains.

The average modes (based on point counting analyses of 5–7 samples; Frindt et al., 2004a) and some petrographic characteristics of the Gross Spitzkoppe granites are listed in Table 1. Biotite in all of the granites is siderophyllite and contains 2–3 wt.% F (Frindt et al., 2004a). It is present as subhedral aggregates or is interstitial between quartz and feldspar grains. Biotite is generally relatively well preserved, but in places it is partly replaced by chlorite and white mica. Topaz is found as magmatic subhedral or anhedral grains, and as secondary very small grains replacing plagioclase. Minor fluorite is present in all the granites. Columbite, magnetite, zircon, monazite, thorite, and niobian rutile are characteristic accessory heavy minerals.

Miarolitic cavities are present in all the granites and are most common in the marginal and porphyritic granites. Most of the cavities are a few millimeters or centimeters in size, but pegmatite-lined druses may be over 1 m in diameter (Fig. 3b). The latter contain quartz, K-feldspar, and biotite as well as gem-quality topaz and beryl crystals. Due to reactions with hydrothermal fluids, the porphyritic granite has locally altered to wolframite-bearing greisen (Frindt and Poutiainen, 2002; Frindt et al., 2004a).

4.2. The Klein Spitzkoppe stock

The Klein Spitzkoppe stock (Kandara, 1998) is located in the Damara belt (metasediments, S-type granites and pegmatites) about 15 km west of the Gross

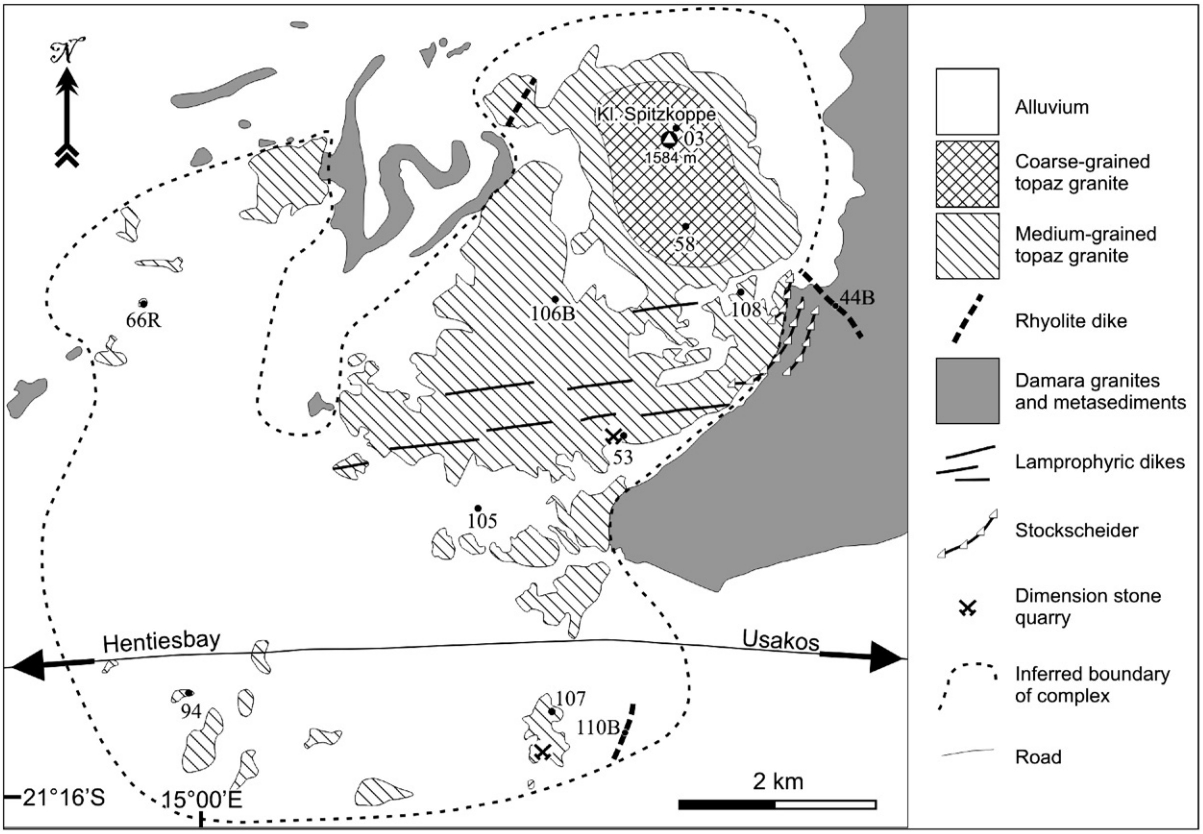

Fig. 4. Geological map of the Klein Spitzkoppe granite stock, modified from Kandara (1998).

Spitzkoppe (Figs. 1 and 4). The northeastern part of the stock comprises the Klein Spitzkoppe mountain that rises about 600 m above the ground level and is well exposed, the southern and western parts of the stock are covered by soil (gravel, sand) and calcrete. The stock consists of two main granite types: a coarse-grained granite that forms the mountain, and a surrounding equigranular or porphyritic medium-grained granite. The contacts between the granite types are commonly gradational, in places sharp. The irregular (flat?) western contact with the Damara country rocks and the abundant occurrence of miarolitic cavities (in places interconnected) and larger pegmatite-lined druses in the medium-grained granite suggest that wide areas of the flat-lying medium-grained granite represent roof facies of the pluton. The main granites are cut by microgranite dikes, a few rhyolite dikes, and east-trending lamprophyre dikes. In the eastern margin of the stock, a gently outward dipping dike-like layered pegmatite–aplite stockscheider is exposed (Fig. 3d). The miarolitic cavities and pegmatite pockets are known of their gem-quality topaz and beryl crystals, and locally also phenacite and bertrandite are found in the pegmaties (Ramdohr, 1941). A few greisen veins are found in the medium-grained granite, and near the northern margin of the stock there is in the granite a hydrothermally altered zone with Cu–As–Fe sulphide and cassiterite mineralization (Frommurze et al., 1942).

The main petrographic features of the Klein Spitzkoppe granites are summarized in Table 1. The granites are syenogranites and show little modal variation. According to point counting analyses by Kandara (1998), perthitic alkali feldspar, quartz, and albitic plagioclase make up around 95 vol.% of the rock, the remainder is annite–siderophyllite (2–4 vol.%), topaz (1 vol.%), and fluorite (1 vol.%). Typical accessory heavy minerals include columbite, zircon, monazite, ilmenite, magnetite, and rutile. Biotite is generally relatively homogenous and well preserved, but in places partly replaced by white mica and secondary iron oxide. Biotite and topaz have a similar mode of occurrence as in the Gross Spitzkoppe granites.

4.3. Geochemistry of the Spitzkoppe granites

Only small geochemical differences are found among the texturally distinct types of the Gross Spitzkoppe stock (Frindt et al., 2004a); this applies also to the granites of the Klein Spitzkoppe stock. The average compositions of the two stocks are nearly identical (Table 2).

The Gross and Klein Spitzkoppe granites are marginally peraluminous (A/CNK in Gross Spitzkoppe granites 0.95 to 1.06, in Klein Spitzkoppe granites 1.00 to 1.09), highly evolved granites. They are characterized by high SiO_2 (74.4 to 78.6 wt.% in Gross Spitzkoppe, 75.8 to 77.8 in Klein Spitzkoppe) and high Na_2O+K_2O (7.6 to 8.8 wt.% in Gross Spitzkoppe, 7.9 to 8.8 wt.% in Klein Spitzkoppe) with K_2O prevailing over Na_2O. Characteristic are also high Fe/Mg, K, Rb, Ga and F, as well as very low TiO_2, MgO, Ba, Sr, and P. High Rb/Sr (in Gross Spitzkoppe 12 to 122 with a mean at 38, in Klein Spitzkoppe 17 to 53 with a mean at 38) indicates highly evolved magmas. The average *F* content in the Gross Spitzkoppe granites is 0.47, in Klein Spitzkoppe 0.49. The boron content is always low, less than 10 ppm. Interestingly, elevated *F* contents seem to be characteristic for the various rock types of the Damaraland intrusive complexes.

Some differences between the granites of the two stocks are evident in their REE patterns (Fig. 5). The sum of REEs varies in Gross Spitzkoppe from 109 to 625 ppm (mean at 407 ppm) and in Klein Spitzkoppe from 195 to 352 ppm (mean at 254 ppm). The Gross Spitzkoppe granites, especially the coarse-grained and porphyritic types, are enriched in the light REEs having $(La/Yb)_N$ 2.5 to 7.7 (mean 4.4), whereas the Klein Spitzkoppe granites have $(La/Yb)_N$ of 0.6 to 1.6 (mean 0.9). The negative $(Eu/Eu^*)_N$ anomaly is, in average, deeper in the Klein Spitzkoppe granites (range 0.07 to 0.38, mean 0.14) than in the Gross Spitzkoppe granites (range 0.0 to 0.47, mean 0.26). The REE tetrad effect, which is characteristic of highly evolved volatile-rich granites and reflects the residual melt–aqueous fluid interaction (Irber, 1999; Jahn et al., 2001; Monecke et al., 2002), is slightly more pronounced in the Klein Spitzkoppe granites than in the Gross Spitzkoppe granites (Table 2; Fig. 5). Zr/Hf and Nb/Ta decrease from the Gross Spitzkoppe to Klein Spitzkoppe granites. These observations indicate that the visible part of the Klein Spitzkoppe stock contains slightly more evolved granites than the Gross Spitzkoppe stock. This conclusion is supported also by Zr contents and zircon saturation model temperatures (Watson and Harrison, 1983) that are slightly lower in the Klein Spitzkoppe granites (Zr 138 to 230 ppm with a mean at 178 ppm, T 782 to 822 °C with a mean at 798 °C) than in the Gross Spitzkoppe granites (Zr 74 to 306 ppm with a mean at 225 ppm, T 740 to 851 °C with a mean at 816 °C). The slightly more evolved geochemical character of the Klein Spitzkoppe granites may be related to the widespread presence of volatile-enriched roof facies granites (higher erosional section) in the Klein Spitzkoppe stock.

In the geochemical discrimination diagrams of Whalen et al. (1987) and Pearce et al. (1984), the Gross and Klein Spitzkoppe granites plot in the fields of A-type and within plate granites (Fig. 6a–d). The granitic rocks of the other silicic Damaraland intrusive complexes (Erongo, Brandberg, Messum, Cape Cross, Paresis) share these characteristics. This is quite interesting in view of the fact that isotopic compositions suggest different sources for these granites. In the Ga/Al versus Zr+Nb+Y+Ce diagram (Fig. 6a), the Erongo granites plot into the FG field; this is common for many fractionated felsic granites of different types (Whalen et al., 1987; Eby, 1990). In the classification scheme of Frost et al. (2001), the Spitzkoppe granites are ferroan alkali-calcic granites.

5. Isotope geochemistry and petrogenetic interpretations of the Etendeka volcanic and Damaraland intrusive complexes

The Damaraland intrusive rocks and the Etendeka lavas are contemporary and cospatial. In this section we review the published O, Nd and Sr isotopic data on the silicic complexes (Table 3, Fig. 7) and the petrogenetic interpretations that have been proposed for these rocks.

5.1. The Etendeka lavas

The geochemistry, isotope geochemistry and petrogenesis of the Paraná–Etendeka lava series have been studied in numerous papers, and various petrogenetic models have been proposed for the observed magma types (see, e.g., Garland et al., 1995; Ewart et al., 2004a,b and references therein). It is a question of a huge, heterogeneous multicomponent magmatic system, and exact petrogenetic modeling of individual magma types is very difficult and highly uncertain.

Initial isotopic compositions that closely correspond to the Tristan hot spot mafic lavas (ε_{Nd} around 0; $^{87}Sr/^{86}Sr$ 0.704–0.705) have been obtained for a few volcanic units, including the Tafelkop basalts north of the Messum complex, the Messum basanite dikes (Harris et al., 1999), and some ferropicrite dikes and associated lavas (Thompson et al., 2001), as well as alkaline gabbros of the Messum (Harris et al., 1999), Okenyena (Milner and le Roex, 1996) and Erongo

Table 2
Chemical analyses of the Klein Spitzkoppe granites and two rhyolite dikes, compared with the mean composition of Gross Spitzkoppe granites (13 analyses in Frindt et al., 2004a)

Coarse-grained granite				Medium-grained granite							Rhyolite dikes		Mean of Kl.	Mean of Gr.
				Even-grained					Porphyritic		Flow-banded	Porphyritic	Spitzkoppe granites	Spitzkoppe granites
Sample	JK03	JK58	JK100	JK107	JK105	JK66R	JK94	JK53	JK106B	JK108	JK110A	JK44B		
SiO_2	77.8	76.6	77.0	76.3	75.8	76.9	77.8	77.1	75.5	76.3	75.5	76.2	76.71 (0.77)	76.22 (1.16)
TiO_2	0.02	0.01	0.05	0.02	0.08	0.00	0.02	0.02	0.06	0.05	0.10	0.02	0.03 (0.03)	0.09 (0.04)
Al_2O_3	12.6	13.0	12.7	12.5	12.3	13.3	12.2	13.1	12.9	12.9	12.4	13.3	12.75 (0.35)	12.48 (0.33)
Fe_2O_3	0.39	0.62	0.70	0.36	0.78	0.39	0.50	0.44	0.59	0.64	0.89	0.08	0.54 (0.15)	0.60 (0.60)
FeO	0.50	0.10	0.50	0.60	1.00	0.30	0.60	0.20	0.70	0.70	1.10	0.20	0.52 (0.27)	0.80 (0.34)
MnO	<0.01	<0.01	0.01	0.01	0.03	<0.01	0.01	0.02	0.02	0.02	0.01	<0.01	0.01 (0.01)	0.01 (0.01)
MgO	<0.01	<0.01	<0.01	<0.01	<0.01	<0.01	<0.01	<0.01	<0.01	<0.01	<0.01	<0.01	<0.01	0.01 (0.03)
CaO	0.32	0.43	0.28	0.55	0.63	0.31	0.54	0.20	0.74	0.75	0.56	1.54	0.48 (0.20)	0.54 (0.24)
Na_2O	3.94	4.11	3.80	4.01	3.33	4.17	4.03	4.48	3.75	3.69	3.23	4.22	3.93 (0.31)	3.42 (0.29)
K_2O	4.17	4.47	4.74	4.40	5.11	4.57	3.84	3.97	5.03	4.59	5.66	4.30	4.49 (0.42)	5.01 (0.48)
P_2O_5	<0.01	<0.01	0.04	<0.01	<0.01	<0.01	<0.01	<0.01	<0.01	<0.01	<0.01	<0.01	<0.01	0.04 (0.06)
F	0.49	0.35	0.39	0.43	0.53	0.31	0.52	0.50	0.67	0.72	0.30	0.67	0.49 (0.13)	0.47 (0.17)
LOI	0.35	0.85	0.35	0.35	0.40	0.15	0.40	0.25	0.45	0.45	0.45	0.30	0.40 (0.18)	0.46 (0.16)
Subtotal	100.58	100.54	100.56	99.53	99.99	100.40	100.46	100.28	100.41	100.81	100.20	101.05	100.35	100.15
$-O=F_2$	0.21	0.15	0.17	0.18	0.22	0.13	0.22	0.21	0.28	0.30	0.13	0.28	0.21 (0.05)	0.20 (0.07)
Total	100.37	100.39	100.39	99.35	99.77	100.27	100.24	100.07	100.13	100.51	100.07	100.77	100.14	99.95
A/CNK	1.09	1.05	1.07	1.01	1.01	1.08	1.04	1.09	1.00	1.04	1.00	0.92	1.05	1.04
ppm														
Cl	197	10	188	215	263	103	172	100	246	204	544	142	170 (77)	230 (110)
Be	4	3	4	5	4	4	6	8	4	4	7	9	4.6 (1.4)	6.4 (2.9)
Li	212	194	175	128	175	103	127	232	125	184	84	28	66 (43)	135 (34)
Rb	728	822	688	589	649	739	562	957	575	648	487	467	696 (123)	604 (131)
Cs	10	5	9	7	11	8	10	15	7	13	4	3	9.5 (3.0)	8.2 (2.6)
Sr	16	23	39	14	13	16	19	18	15	27	18	88	20 (8)	21 (11)
Ba	22	120	50	24	78	25	20	20	32	46	31	288	44 (33)	85 (44)
Ga	42	54	40	43	38	49	41	52	31	34	48	47	42 (7)	34 (6)

Y	191	113	173	176	205	117	256	66	155	150	109	192	160 (53)	131 (72)
Zn	47	37	49	48	81	25	44	43	62	56	89	11	49 (15)	41 (10)
Zr	198	147	175	166	175	172	179	138	195	230	381	188	178 (26)	221 (66)
Hf	8.6	7.5	7.9	8.6	6.0	15.0	8.4	11.0	7.5	7.7	14	10	8.8 (2.5)	8.4 (1.0)
Sn	32	27	29	17	42	10	12	43	18	16	14	8	25 (12)	12 (6)
Nb	41	45	81	60	96	54	56	43	94	88	266	97	66 (22)	92 (21)
Ta	13	14	13	13	14	14	15	20	11	15	10	19	14 (2)	9.5 (3.7)
W	3	3	5	3	3	3	4	4	7	5	5	5	4 (1)	3.7 (1.7)
U	7	9	20	8	9	5	7	6	9	10	9	5	9 (4)	17 (8)
Th	42	26	49	54	54	42	55	27	58	55	77	63	46 (12)	70 (30)
Pb	26	9	69	35	51	35	42	53	43	36	30	30	40 (16)	22 (9)
La	22.8	21.1	32.8	20.4	35.3	25.8	38.8	19.4	42.9	44.6	93.1	45.8	30.4 (9.7)	81.3 (36.1)
Ce	64.8	56.2	80.4	52.3	88.6	74.3	101.0	64.1	95.8	101.0	182.0	107.0	77.9 (18.3)	163 (65)
Pr	9.1	7.6	10.6	7.5	11.7	10.3	13.6	7.6	11.7	12.4	18.1	12.8	10.2 (2.2)	17.8 (6.8)
Nd	37.6	28.9	41.7	31.3	47.9	41.4	55.5	26.5	44.7	46.5	58.7	45.5	40.2 (9.2)	59.9 (23.6)
Sm	13.9	10.5	14.6	12.3	17.1	15.8	20.7	9.8	13.9	13.6	14.3	14.0	14.2 (3.2)	14.7 (6.5)
Eu	0.06	0.05	0.21	0.07	0.14	0.05	0.05	0.05	0.26	0.33	0.26	0.14	0.13 (0.10)	0.22 (0.16)
Gd	12.5	9.4	14.3	12.6	16.5	12.5	20.9	7.3	13.9	12.5	13.4	12.3	13.2 (3.7)	13.3 (6.4)
Tb	2.7	2.1	2.9	2.6	3.3	2.8	4.2	1.7	2.7	2.5	2.9	2.7	2.8 (0.7)	2.6 (1.2)
Dy	19.0	15.3	20.8	18.4	23.0	19.5	28.8	12.8	19.0	17.8	28.8	18.8	19.4 (4.3)	17.7 (9.0)
Ho	4.38	3.57	4.78	4.37	5.42	4.35	6.63	2.83	4.43	4.21	5.12	4.32	4.50 (1.01)	4.0 (2.2)
Er	16.0	13.1	15.9	14.7	18.5	16.0	23.1	10.9	14.8	14.0	17.2	15.0	15.7 (3.3)	13.7 (6.8)
Tm	3.1	2.8	2.9	2.8	3.3	3.3	4.3	2.5	2.5	2.5	2.8	2.9	3.0 (0.5)	2.39 (1.14)
Yb	25.0	22.8	21.8	21.0	24.4	29.5	33.1	22.6	17.8	18.7	18.5	22.0	23.7 (4.7)	13.6 (6.5)
Lu	3.87	3.62	3.35	3.33	3.81	4.76	5.18	3.45	2.61	2.86	2.59	3.41	3.68 (0.79)	2.6 (1.26)
$(La/Yb)_N$	0.62	0.63	1.02	0.66	0.98	0.59	0.79	0.58	1.63	1.61	3.39	1.41	0.91	4.44
Eu/Eu*	0.07	0.07	0.23	0.08	0.14	0.05	0.05	0.07	0.29	0.38	0.06	0.16	0.14	0.26
Ce/Ce*	1.15	1.15	1.08	1.06	1.08	1.18	1.10	1.42	1.05	1.07	1.09	1.12	1.12	1.10
Pr/Pr*	1.13	1.15	1.09	1.09	1.07	1.15	1.09	1.26	1.05	1.07	1.04	1.11	1.10	1.08
TE1	1.14	1.15	1.08	1.08	1.08	1.16	1.10	1.34	1.05	1.07	1.07	1.11	1.11	1.09

Eu/Eu* = $Eu_N/Sm_N \cdot Gd_N$, Ce/Ce* = $Ce_N/(La_N^{2/3} \cdot Nd_N^{1/3})$, Pr/Pr* = $Pr_N/(La_N^{1/3} \cdot Nd_N^{2/3})$, degree of the tetrad effect: TE1 = $(Ce/Ce^* \cdot Pr/Pr^*)^{1/2}$, numbers in parentheses are 2σ standard deviation. LOI = loss of ignition. The analyses were made by X-ray Assay Laboratories (Canada) using XRF (major oxides, Rb, Ba, Zr, Nb, Y), ICP-MS (REE, Ga, Sn), ICP (Be, Sr, Zn, Pb), NA (U, Th, Ta, W, Hf), and wet chemical (FeO, F, Cl) methods. Fe_2O_3 values calculated from Fe_2O_3 (total iron; XRF) and FeO (wet chemical) contents.

(Trumbull et al., 2003) complexes. Most of the Etendeka–Paraná mafic lavas have negative ε_{Nd} values (−3 to −9; Fig. 7) and varying initial $^{87}Sr/^{86}Sr$ (0.707 to 0.712; Ewart et al., 1998a, 2004a); this has been attributed to sublithospheric or enriched subcontinental lithospheric mantle (SCLM) source components (e.g., Peate and Hawkesworth, 1996; Gibson et al., 1995; Hawkesworth et al., 1999) or to crustal contamination of the mantle magmas (Milner and le Roex, 1996; le Roex and Lanyon, 1998).

In a recent study, Ewart et al. (2004a,b) re-evaluated the petrogenesis of the Etendeka mafic and silicic lavas. For the mafic lavas they assumed three sublithospheric source components [Tristan OIB as plume-derived melt; N-MORB as depleted asthenospheric melt; Gaussberg lamproite composition (Murphy et al., 2002) — an inferred product of recycling of subducted sedimentary slab stored in the Transitional Zone] and GLOSS (global subducting sediment average; Plank and Langmuir, 1998) as a crustal component. According to Ewart et al., the geochemical and isotopic composition of the mafic lavas can be explained without invoking a significant SCLM component. They suggested that entrainment of remnants of a pre-existing metasediment-bearing subducted slab within the Transitional Zone during plume ascent was the main reason for the geochemical and isotopic crustal-sediment component of the mafic mantle lavas. Numerical modeling of the mafic lavas (basalts, andesites) by Ewart et al. (2004a) implies that the Khumib–Urubici high-Ti basalts have a major plume component and subordinate N-MORB and recycled subducted ancient sedimentary (+MORB) components. The Tafelberg–Gramado-type low-Ti lava series has a strong crustal (GLOSS) component and significant N-MORB input as well as subordinate plume and subducted sediment components, whereas the Tafelkop lavas have a major Tristan plume component with important N-MORB component and a minor subducted sediment component. The Horinbaai-type magmas contain a major (>85%) N-MORB component and a minor Tristan plume component.

The modeling of Ewart et al. (2004a) is an alternative for the commonly applied SCLM model, but it does not exclude SCLM as a possible source component of the Etendeka and Damaraland magmas. It is possible that some enriched SCLM component (e.g., alkali metasomatized mantle, mantle containing relicts of a Neoproterozoic subducted slab) was incorporated into the plume melts during plume's ascent to the base of the lithosphere.

Like the mafic lavas, the Etendeka silicic lavas (minor latite, voluminous quartz latite) can be divided into high-Ti and low-Ti types, and the major and trace element composition of the high-Ti lavas shows typical magmatic evolution trends with increasing SiO_2. The low-Ti quartz latites are the most evolved lavas with high Rb, Cs, Th, U, Pb and Li and low Ba and Sr. They have stronger negative Eu anomalies and lowered La/Yb and Nb/Ta (Ewart et al., 2004b). The initial $^{87}Sr/^{86}Sr$ and ε_{Nd} values for the high-Ti silicic lavas are 0.706 to 0.71 and −3.8 to −6.7, respectively; for the low-Ti quartz latites, these parameters are 0.72 to 0.725 and −7.8 to −8.6. The origin and evolution of the silicic eruptive rocks have been a matter of debate, the principal postulated mechanisms being (1) crustal contamination of mantle magmas, combined with fractional crystallization (AFC-processes) and (2) partial melting caused by magmatic underplate with a varying mantle input. The numerical modeling by Ewart et al. (2004b) suggests various combinations of ACF-style processes

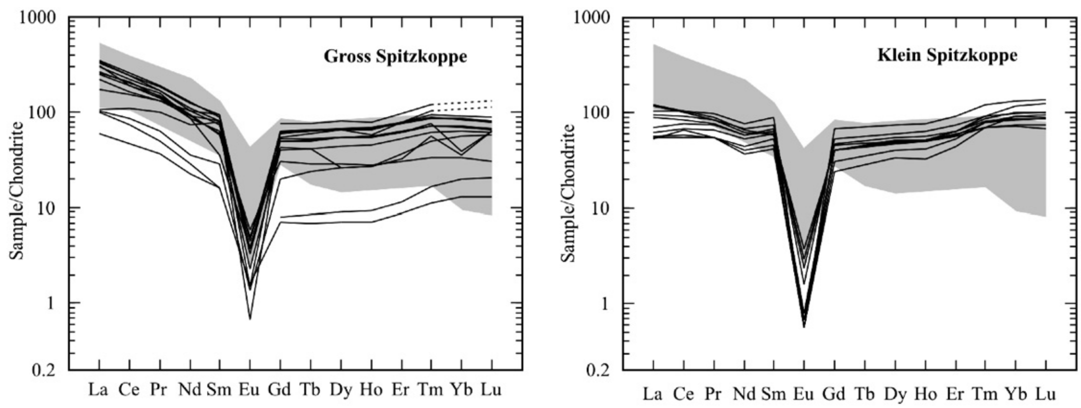

Fig. 5. Chondrite-normalized (Boynton, 1984) REE distribution diagrams for the Gross Spitzkoppe and Klein Spitzkoppe granites. Shaded background denotes the field of Finnish rapakivi granites (Haapala et al., 2005).

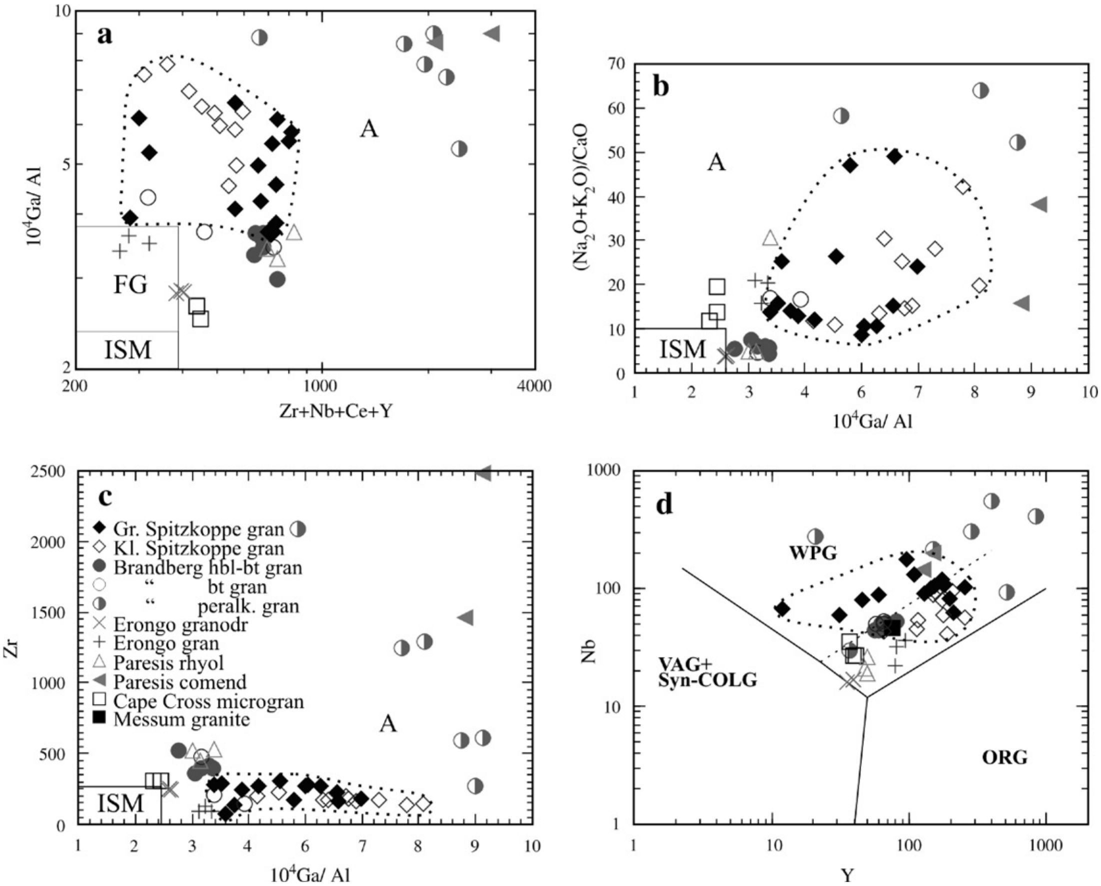

Fig. 6. Analyses of Gross Spitzkoppe and Klein Spitzkoppe granites (Kandara, 1998; Frindt et al., 2004a) and other silicic rocks of the Cretaceous Damaraland complexes (Schmitt et al., 2000; Trumbull et al., 2000, 2003, 2004) in the geochemical discrimination diagrams of Whalen et al. (1987), Eby (1990), and Pearce et al. (1984). FG = field of fractionated granites where several fractionated granites of different alphabetic types plot; WPG = within plate granites, ORG = ocean ridge granites, VAG = volcanic arc granites, Syn-COLG = syn-collisional granites.

and magma mixing for the high-Ti latites and quartz latites, but cannot exclude partial melting as an alternative process. The geochemically more evolved low-Ti quartz latites need a massive crustal component and their formation may involve voluminous (large-degree) partial melting of crustal sources and large-scale AFC-processes (see Ewart et al., 2004b), or partial melting of crustal rocks (granulite, basalt) with input of mantle component (e.g., Harris et al., 1990; Garland et al., 1995; Trumbull et al., 2004).

5.2. The Damaraland granitic rocks

From the geological context and geochemical and isotopic data (Fig. 7) it is obvious that the Damaraland granites have three main sources: mantle magmas, Damara crust, and pre-Damara basement. Each of these sources shows wide compositional variation. Trumbull et al. (2004) compared the $\delta^{18}O$ values versus initial (130 Ma) ε_{Nd} and $^{87}Sr/^{86}Sr$ values of the Damaraland granitoids (Paresis excluded) and their possible sources. For the sources they used (1) the Tristan hot spot alkaline basalts, (2) the average of the widespread peraluminous S-type Damara granites with metasedimentary source, and (3) the average of the less voluminous post-tectonic metaluminous–peraluminous A-type Damara granites whose source has been attributed to intermediate-felsic lower crust (Jung et al., 2000, 2001). The Cretaceous Damaraland granites plotted inside the triangle defined by these postulated sources and, in accordance with some earlier studies (e.g., Harris, 1995; Frindt et al., 2004b), Trumbull et al. concluded that the crustal source component was dehydrated and possibly melt-depleted lower crustal metasediments and the mantle component was dominated by the Tristan mantle plume. The $\delta^{18}O$ versus ε_{Nd} data of Trumbull et al. (2004) suggested also involvement of a depleted mantle component in some of the

Table 3
Main (silicic) rock types and their isotopic characteristics in some Damaraland igneous complexes

Complex	Rocks	Al saturation	Age Ma	Method	$\varepsilon_{Nd\,i}$	$\delta^{87}Sr/^{86}Sr_i$	$\delta^{18}O_{quartz}$	$\delta^{18}O_{magma}$	Ref.
Gross Spitzkoppe	Bt–tz granites	Peraluminous (metaluminous)	125±1	Rb–Sr	−5.6 to −6.4	0.710–0.716	11.8–12.6	10.0–10.8	(1,2)
Klein Spitzkoppe	Bt–tz granites	Peraluminous					12.0	10.0	(3)
Erongo	Rhyodacite		135±3	U–Pb					(4)
	Granodiorite	Peraluminous	132±3	Ar–Ar	−9.0 to −9.3	0.726–0.729	12.4	10.4	(2)
	Bt–to granite	Peraluminous			−6.9 to −8.7		12.0–12.3	10.0–10.3	(2)
Brandberg	Bt–hbl granite	Metaluminous	133±2	Ar–Ar	−2.6 to −3.2	0.712–0.712	10.1–10.8	8.1–8.8	(2,5)
	Bt granite	Metaluminous			−2.4	0.706			
	Arfv. granite	Peralkaline	132±2	Ar–Ar	−0.8 to −1.9		10.5–10.8	8.5–8.8	(2,5)
Messum	Gabbro	Tholeiitic	131.7±0.7 132.1±1.2	Ar–Ar Ar–Arf	+3.9, −12	0.704–0.710			(7,10)
	Neph. gabbro	Alkaline			+2.07	0.705		6.8	(8)
	Neph. syenite	Alkaline	129.3±0.7	Ar–Ar	+1.7 to +2.6	0.705–0.706	9.2, 9.4	6.0–6.8	(7,8,10)
	Quartz syenite	Metaluminous			+1.7 to −3.1	0.706–0.710	9.8	7.2, 7.4	(7,8)
	Granite (HC 74)	Metaluminous			−0.6	0.708		7.8	(8)
Cape Cross	Gabbro								
	Microgranite	Metaluminous–peraluminous	135±0.7	Ar–Ar	−4.1 to −4.7	0.722–0.727			(2,6)
	Neph. syenite	Alkaline			−5.6 to −6.4	0.710–0.716			(2)
Paresis	Rhyodacite and rhyolite	Metaluminous–peraluminous	137±1	Ar–Ar	−20.5 to −21.3	0.712–0.714	10.0	9.0	(6,9)
	Comendite	Peralkaline–peraluminous	134±2	U–P	−10.8, −11.3				(7,9)
	Quartz syenite	Metaluminous			−9.5, −9.6	0.707,0.709			(7,9)

(1) Frindt et al. (2004b); (2) Trumbull et al. (2004); (3) Harris (1995); (4) Pirajno et al. (2000); (5) Schmidt et al. (2000); (6) Milner et al. (1995); (7) Trumbull et al. (2000); (8) Harris et al. (1999); (9) Mingram et al. (2000); (10) Renne et al. (1996).

mantle magmas, but "ruled out" a significant role of enriched SCLM component.

The available ε_{Nd} versus $^{87}Sr/^{86}Sr$ (Fig. 7) and ε_{Nd} versus $\delta^{18}O$ data (Trumbull et al., 2004) indicate roughly similar mantle–crust mixing relations for the main Damaraland granite complexes, in order of increasing crustal source component: Brandberg (and Messum) metaluminous granites – Gross Spitzkoppe topaz granites – Erongo granitoids (granodiorite, granite). This evolution trend follows and overlaps the evolution of Etendeka low-Ti volcanic rocks (Tafelkop basalts – Tafelberg basalt series – quartz latites; Fig. 7). Obviously, the lavas and granitoids had similarities in their petrogenesis, although they crystallized in different conditions and, in general, differ from each other in geochemical composition. In an intracrustal magma chamber, closed and open system magmatic differentiation processes may produce a variety of rocks from the parent magma.

Isotopic data suggest that the metaluminous biotite–hornblende granites (and the minor peralkaline granites) of Brandberg have dominant mantle source components, corresponding the Tafelberg low-Ti basalts, and their origin has been modeled as crustally contaminated (20–40%) fractionate of tholeiitic low-Ti basalt (Schmitt et al., 2000). The more mafic and slightly earlier monzonites of the Brandberg pluton have more primitive initial isotopic composition (ε_{Nd} −0.4, −0.7; $^{87}Sr/^{86}Sr$ 0.707, 0.708). The (metaluminous-) marginally peraluminous Gross Spitzkoppe topaz granites have substantial components of both mantle and crustal sources, with initial isotopic compositions (ε_{Nd} −5.6 to −6.4; $^{87}Sr/^{86}Sr$ 0.710 −0.713) overlapping with the evolved members of the Tafelberg lavas. Although granitic in composition, the Gross Spitzkoppe stock shows strong evidence of bimodal association (synplutonic mafic dikes, magmatic mafic enclaves) as well as magma mingling and mixing. Origin by partial melting of lower crustal melt-depleted granulitic rocks, caused by magmatic underplating, with substantial mantle input and subsequent fractionation, has been suggested (Frindt et al., 2004b). The low content of boron (and absence of tourmaline) in the granite does not imply substantial metasedimentary source component, but high $\delta^{18}O$ (10.0–10.8; Trumbull et al., 2004) suggests significant metasedimentary component. The strongly peraluminous Erongo cordierite-bearing granodiorite as well as the tourmaline- and topaz-bearing granite, which

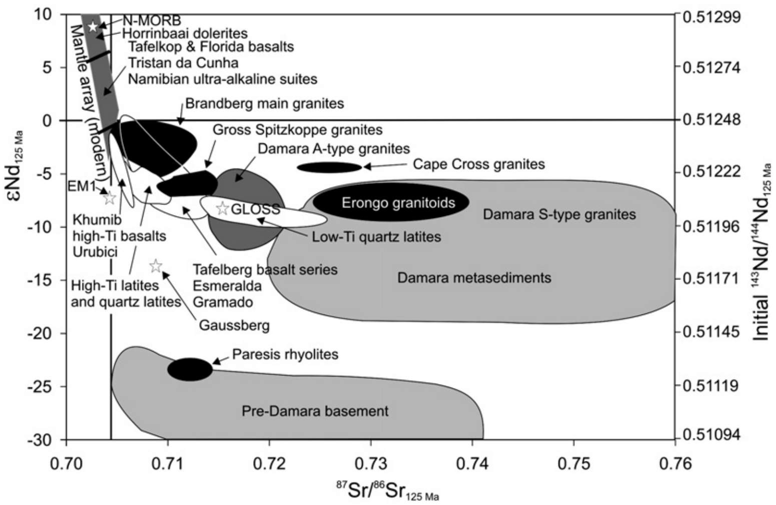

Fig. 7. Initial Nd–Sr isotopic compositions of the Cretaceous Damaraland igneous complexes and Etendeka volcanic series (with some volcanic series from Paraná). The diagram is based on data presented in Frindt et al. (2004b; calculated at 125 Ma) and Ewart et al. (2004a,b; initial values at 132 Ma). Recalculation of the Nd and Sr initial ratios of Ewart et al. (1998a,b, 2004a,b) for 125 Ma leads to insignificant changes in the initial ratios (±0.0002), and the fields were drawn directly from the data of Fig. 12 of Ewart et al. (2004a). The compositions of Gaussberg lamproites (Murphy et al., 2002) and GLOSS (global sediment average; Plank and Langmuir, 1998) as well as the centres of the enriched mantle (EM 1) and N-MORB fields are indicated. Data sources: Frindt et al. (2004b) (Gross Spitzkoppe granites); Trumbull et al. (2000, 2004) (Erongo granitoids); Schmitt et al. (2000) (Brandberg granites); Trumbull et al. (2004) (Cape Cross granites); Trumbull et al. (2004) (Paresis rhyolites); Ewart et al. (1998a,b, 2004a,b) (the fields of the Etendeka–Paraná volcanic series and mafic-alkaline intrusive rocks); McDermott and Hawkesworth (1990) (Damara metasediments); McDermott et al. (1996) and Jung et al. (2001) (the fields of Damara S-type granites); Jung et al. (1998) and McDermott et al. (2000) (Damara A-type granites), and Seth et al. (1998) (pre-Damara basement).

overlap in initial isotopic composition (ε_{Nd} −6.9 to −9.3; $^{87}Sr/^{86}Sr$ 0.726–0.729, $\delta^{18}O$ 10.0–10.4) with the Damara metasediments and granites, has been attributed to melting of lower crustal metasedimentary rocks (Trumbull et al., 2000, 2004). Interestingly, small basanite–tephrite plugs of the Erongo complex have plume-like initial isotopic compositions (ε_{Nd} +1.8 to +2.7; $^{87}Sr/^{86}Sr$ 0.704–0.705) (Trumbull et al., 2003).

The only available isotope analysis of a granitic member of the Messum core quartz syenite suite (ε_{Nd} −0.6; $^{87}Sr/^{86}Sr$ 0.708; $\delta^{18}O$ 7.8‰) deviates only slightly from the plume-like composition of the nepheline syenites, and the quartz syenite–granite suite may be formed from the nepheline syenite magma by crustal assimilation (Harris et al., 1999). Unfortunately, no isotope analyses are available of the more voluminous granitic rocks of the outer zone of the Messum complex. The Cape Cross ring complex has markedly lower initial ε_{Nd} values (−4.1 to −4.7) and higher $^{87}Sr/^{86}Sr$ values (0.722–0.727), suggesting substantial crustal (metasedimentary?) source component.

The Paresis silicic complex deviates markedly from the other Damaraland anorogenic complexes (Mingram et al., 2000). It intrudes Damara metasediments but is located close to the margin of the pre-Damara basement (Congo craton), where also large basement inliers occur in the Damara belt, suggesting that the craton slopes below the Damara metasediments. Initial (132 Ma) ε_{Nd} and $^{87}Sr/^{86}Sr$ values in the metaluminous–peraluminous rhyodacites and rhyolites are −20.5 to −21.3 and 0.712–0.714, respectively, corresponding to the pre-Damara basement gneisses; the peralkaline comendites and metaluminous quartz syenites have ε_{Nd} values at −9.5 to −11.3 and the slightly alkaline basalt, phonolite and lamprophyre show ε_{Nd} of −0.9 to −2.8 and $^{87}Sr/^{86}Sr$ of 0.704–0.705, approaching plume composition. The comendites and quartz syenites are interpreted as hybrids between crustal and mantle-derived components (Mingram et al., 2000).

6. Discussion: origin of the A-type granites

The main models presented for the origin of A-type granites and rhyolites can be listed as follows:

(1) Fractional crystallization of mafic, mantle-derived magmas, with or without substantial assimilation of crustal rocks (AFC-style processes). This model has been applied particularly to peralkaline granites and rhyolites (e.g., Peccarillo et al.,

2003), but also to other A-type silicic rocks (Bonin, 1998; Ewart et al., 2004b), and some experimental studies support it (Nekvasil et al., 2004). The model requires extreme fractionation, which may be possible by magmatic differentiation in one or several, progressively shallower magma chambers, prior to the final emplacement of the magma (Bonin, 1998).

(2) Partial melting of pre-existing rocks by mantle-derived magmatic underplate, commonly with input of mantle material. On the basis of the geological history and character of the melting rock, three modifications can be delineated:
   (a) Partial melting of metaigneous or metasedimentary lower or mid-crustal rocks that have been melt-depleted in previous partial meltings. This is a widely used model (e.g., Emslie, 1978; Collins et al., 1982; Anderson and Bender, 1989; Haapala and Rämö, 1990), and it has been supported by chemical and physical modelings (Clemens et al., 1986; Huppert and Sparks, 1988). A problem with this model is that, in several instances, the ε_{Nd} values of the granites and associated mafic, presumably mantle-derived rocks largely overlap.
   (b) Partial low-degree melting of a juvenile mafic underplate, variously fractionated and hybridized with older crustal rocks, by repeated injections of mantle magmas (Hildreth et al., 1991; Frost and Frost, 1997). This model explains the reduced character of most A-type granites and the isotopic similarities of several granite–gabbro/diabase associations.
   (c) Partial (or near-complete) melting of lower crust that was alkali metasomatized by fluids derived by mantle degassing in rift zones (Martin, 2006). Areas undergoing extension above upwelling asthenospheric mantle are loci of mantle degassing and subsequent melting. The emanating fluids (H_2O, CO_2, CH_4, F, Cl) are alkali and silica bearing and able to transport a variety of elements, including high-field-strength and rare earth elements, and metasomatize the upper mantle (Woolley, 1987) and lower crust (Martin, 2006). Fenitization-type reactions can transfer the refractory (granulitic) mafic–intermediate lower crust to a fertile assemblage that can melt to produce A-type metaluminous or peralkaline granite and alkaline rock magmas. The isotopic composition of such granite would be reset to a blend of crustal signatures and a mantle contribution. Subsequent degassing and preferential loss of alkalies from crystallizing epizonal granite magmas may produce peraluminous granites (Martin, 2006).

In evaluating whether one or more of these models may explain the origin of the Damaraland granites, it is necessary to remember that these complexes include also differentiated mafic and alkaline ring complexes as well as carbonatites. Another feature that may be of importance is the subsurface structure of the Messum and Cape Cross complexes (Bauer et al., 2003). Geophysical data indicate that these ring complexes continue as cylinder-like zones down to the mantle–crust boundary. Thus, at least in these two mafic–felsic ring complexes, the magmas penetrated the crust until the upper crust and surface in several pulses, without residing in intracrustal magma chambers in which effective magmatic differentiation could have taken place (see Bonin, 1998). If the geophysical interpretations are right, the lower crustal roots of the complex consist essentially of gabbroic rocks, yet on the surface the complex contains substantial amounts of granitoids and syenites. The isotopic composition of the alkaline rocks and quartz syenite–granite of the Messum core suggest mantle source with crustal assimilation. This invokes surprisingly effective magmatic differentiation during the ascent of the magma pulses through the crust. On the other hand, the seismic structure and composition of the deepest roots of the Messum complex are poorly defined (Bauer et al., 2003), and no isotope data are available from the felsic rocks of the outer zones.

The mafic-alkaline and carbonatite complexes have geochemical and isotopic compositions indicating plume-derived origin with some crustal contamination. In the case of the Paresis volcanic–subvolcanic complex, the rhyolites represent partial melting products of the pre-Damara gneisses, the alkaline basalts and related alkaline rocks the plume-derived mantle magmas, and comendites and quartz syenites products of hybridization that presumably took place mainly near the crust–mantle boundary. In the Erongo complex, the alkaline mafic lavas represent mantle-derived magmas and the granitoids mainly crust-derived magmas with a major metasedimentary source component. The largest granite pluton, Brandberg, obviously represents the upper parts of a differentiated upper crustal magma chamber, and dominant mantle-type isotope signatures suggest either derivation from mafic mantle magmas by AFC-processes or partial melting of newly formed hybridized mafic-intermediate zone at the base of the lower crust.

Unfortunately, the deep structure of this pluton is not known. The highly evolved Gross and Klein Spitzkoppe granites may be derived from magmas formed by partial melting deep crustal suite (melt-depleted granulite) with a substantial mantle input, as suggested in previous studies. Another possibility is, however, that the crustal source was a hybrid between juvenile mantle material and Damara lower crustal rocks that was partially melted by new injections of mantle magmas. (The few synplutonic mafic dikes and associated magmatic mafic inclusions may be relicts of these mantle magmas.)

The new model (2c) involving partial melting of alkali metasomatized lower or middle crust is quite interesting. The tectonic environment of Damaraland would be most suitable for such metasomatism (rising mantle plume as a source of heat and mafic magma, deep fractures across the crust to control the mantle degassing, metasomatism, melting, and subsequent emplacement of the magmas), and the great diversity of the magmatic complexes also fits the model. Alkali metasomatism and carbonation of the upper mantle by plume-derived fluids may have contributed to the generation of carbonatites and lamprophyres (le Roex and Lanyon, 1998). However, more concrete evidence for the presence of alkali metasomatized lower crust (e.g., metasomatized crustal xenoliths in mantle magmas) is lacking in the Damaraland complexes.

The Spitzkoppe granites belong to the low-P subtype of topaz granites, characterized by $SiO_2 > 73$ wt.%, $Al_2O_3 < 14.5$ wt.%, $P_2O_5 < 0.1$ wt.%, $\delta^{18}O < 10‰$ (Taylor, 1992; Taylor and Fallic, 1997). The high-P subtype has opposite characteristics, and is interpreted to have a major metasedimentary source component. The low-P subtype of topaz granites, similar to the Spitzkoppe granites, occurs as late-stage intrusive phases in A-type granite plutons, but they are also found in S- and I-type granite batholiths. As examples may be mentioned the classic ~ 300 Ma Zinnwald tin granite cupola at the boundary between Germany and Czech Republic (e.g., Štemprok and Šulcek, 1969), the Eurajoki and Kymi granites in the 1550 to 1650 Ma rapakivi granite complexes of Finland (Haapala, 1997; Haapala and Lukkari, 2005), the 975 to 1000 Ma Younger Granites of Rondonia (Bettencourt et al., 1999), and the 1830 Ma tin-bearing Pitinga rapakivi granite complex (metaluminous amphibole–biotite granite, peraluminous topaz granite, peralkline cryolite granite) in Amazonas, Brazil (Costi et al., 2000; Lenharo et al., 2003). Topaz is present in the peraluminous granites, in the peralkaline granites fluorine is fixed to mica, amphibole, fluorite and cryolite. All these Proterozoic granites are interpreted to have a dominant Paleoproterozoic crustal source with minor mantle component. The Jurassic Younger Granites of Nigeria have also similarities with the Spitzkoppe and other Damaraland granites: plume-related bimodal mafic–felcic association, metaluminous, topaz-bearing peraluminous and peralkaline granites with columbite–cassiterite mineralization. The granite magmas may have been derived from basaltic parent magmas by magmatic differentiation, or by partial melting of the lower crust, the basaltic magmas acting as heat source (Bowden, 1982).

7. Conclusions

The Cretaceous Damaraland intrusive complexes belong to the Paraná–Etendeka Large Igneous Province and form a compositionally heterogeneous group of tholeiitic and alkaline mafic–ultramafic rocks, carbonatites, alkaline felsic rocks, as well as metaluminous, peraluminous and peralkaline A-type granites.

The Spitzkoppe granite plutons are compositionally homogenous, marginally peraluminous topaz granites. Bimodal magmatism is indicated by synplutonic mafic dikes and hybridized magmatic mafic enclaves. The contacts against the Damara country rocks are marked by layered aplite–pegmatite stockscheiders, and various types of schlieren structures demonstrate magma flow in the crystallizing magma chamber. Separation of a fluid phase has led to the formation of miarolitic cavities, up to 2 m in diameter, with gem-quality topaz and beryl crystals. The granites are low-P topaz granites, similar to evolved late-stage phases of many A-type granite plutons.

Isotopic compositions of the Damaraland granites indicate mixed sources, with highly varying mixing ratios between mantle components (magma, fluid) and Damara crust or pre-Damara basement. Different petrogenetic models can be applied to explain the origin of the A-type granites and associated rocks: (1) differentiation of mantle magmas, with varying crustal assimilation, (2) partial melting of melt-depleted lower crustal rocks by magmatic underplate, with or without input of mantle source component, (3) partial melting of juvenile mantle magma–crust hybrid by continued injections of mantle magmas, and (4) partial melting of newly alkali-metasomatized lower crust by mantle magmas. These different models do not necessarily exclude each other, but may operate sequentially or simultaneously. Thus, in the wide Damaraland anorogenic province, alkali metasomatism of the upper mantle may have contributed to the formation of carbonatites and mafic–ultramafic alkaline rocks, and alkali metasomatic alteration of the lower crust may have contributed, with or without subsequent hybridization, to partial melting of the lower crust to produce parent magmas for the A-type granites. Granitic rocks with isotopic signatures approaching primitive mantle magmas may have originated from mantle magmas by combined crustal assimilation and fractional crystallization processes, or by partial melting of a juvenile mafic–intermediate hybrid or metasomatized lower crust. If different processes can produce A-type granite magmas, suitable combination of these processes may do it as well, the unifying factor being the extensional regime and high temperature caused by upwelling mantle magmas.

Acknowledgments

Our research in Namibia was conducted in 1994–1998 as part of the bilateral project between the Geological Survey of Finland and Geological Survey of Namibia, and has then been continued as research project of the University of Helsinki with funding from Academy of Finland in 1998–2000 (project 40674), Centre of International Mobility (CIMO) in 2001, University of Helsinki and Geological Graduate School in 2001–2002, and Alfred Kordelin Foundation in 2006. This support, which has been essential for Stephen Frindt's and John Kandara's work, is highly appreciated. The manuscript was markedly improved by comments and suggestions from Tapani Rämö, Jaana Halla, and two anonymous reviewers, as well as by the editorial comments from Carol Frost, which is cordially acknowledged. We thank Jussi Pokki and Sari Lukkari for the technical assistance in processing the tables and figures of the manuscript.

References

Anderson, J.L., Bender, E.E., 1989. Nature and origin of Proterozoic A-type granitic magmatism in the southwestern United States of America. Lithos 23, 19–52.

Bauer, K., Trumbull, R.B., Vietor, T., 2003. Geophysical images and crustal model of intrusive structures beneath the Messum ring complex, Namibia. Earth and Planetary Science Letters 216, 65–80.

Bettencourt, J.S., Tosdal, R.M., Leite Jr., W.B., Payolla, B.L., 1999. Mesoproterozoic rapakivi granites of the Rondônia Tin Province, southwestern border of the Amazonian craton, Brazil - I. Reconnaissance U–Pb geochronology and regional implications. Precambrian Research 95, 41–67.

Bonin, B., 1998. Alkaline rocks and geodynamics. Turkish Journal of Earth Sciences 7, 105–118.

Bowden, P., 1982. Magmatic evolution and mineralization in the Nigerian Younger Granite Province. In: Evans, A.M. (Ed.), Metallization Associated with Acid Magmatism. John Wiley and Sons, Chichester, pp. 51–61.

Boynton, W.V., 1984. Cosmochemistry of the rare earth elements: meteorite studies. In: Henderson, P. (Ed.), Rare Earth Element Geochemistry. Elsevier, New York, pp. 63–114.

Clemens, J.D., Holloway, J.P., White, A.J.R., 1986. Origin of A-type granite: experimental constraints. American Mineralogist 71, 317–324.

Coffin, M.F., Eldholm, O., 1994. Large Igneous Provinces: crustal structure, dimensions, and external consequences. Review of Geophysics 32, 1–36.

Collins, W.J., Beams, S.D., White, A.J.R., Chappel, B.W., 1982. Nature and origin of A-type granites with particular reference to southeastern Australia. Contributions to Mineralogy and Petrology 80, 189–200.

Costi, H.T., Dall'Agnol, R., Moura, C.A., 2000. Geology and Pb–Pb geochronology of Paleoproterozoic volcanic and granitic rocks of Pitinga Province, Amazonian Craton, northern Brazil. International Geology Review 42, 832–849.

Eby, N., 1990. The A-type granitoids: a review of their occurrences and chemical characteristics and speculations of their petrogenesis. Lithos 26, 115–134.

Emslie, R.F., 1978. Anorthite massifs, rapakivi granites, and late Proterozoic rifting in North America. Precambrian Research 7, 61–98.

Ewart, A., Milner, S.C., Armstrong, R.A., Duncan, A.R., 1998a. Etendeka volcanism of the Goboboseb Mountains and Messum igneous complex, Namibia. Part I: geochemical evidence on early Cretaceous Tristan plume melts and the role of crustal contamination in the Paraná–Etendeka CFB. Journal of Petrology 39, 191–225.

Ewart, A., Milner, S.C., Armstrong, R.A., Duncan, A.R., 1998b. Etendeka volcanism of the Goboboseb Mountains and Messum igneous complex, Namibia. Part II: voluminous quartz latite volcanism of the Awahab magma system. Journal of Petrology 39, 227–253.

Ewart, A., Marsh, J.S., Milner, S.C., Duncan, A.R., Kamber, B.S., Armstrong, R.A., 2004a. Petrology and geochemistry of early Cretaceous bimodal continental flood volcanism of the NW Etendeka, Namibia. Part 1: introduction, mafic lavas and re-evaluation of mantle source components. Journal of Petrology 45, 59–105.

Ewart, A., Marsh, J.S., Milner, S.C., Duncan, A.R., Kamber, B.S., Armstrong, R.A., 2004b. Petrology and geochemistry of early Cretaceous bimodal continental flood volcanism of the NW Etendeka, NAMIBIA. Part 2: characteristics and petrogenesis of the high-Ti latite and high-Ti and low-Ti voluminous quartz latite eruptions. Journal of Petrology 45, 107–138.

Frindt, S., 1997. Petrography and geochemistry of the Gross Spitzkoppe igneous complex, central western Namibia. Unpublished M. Sc. thesis, Department of Geology, University of Helsinki.

Frindt, S., Haapala, I., 2002. The Cretaceous Gross Spitzkoppe granite stock in Namibia, a highly evolved A-type granite with structures and textures demonstrating magma flow, undercooling and vapor saturation during crystallization. 11th Quadrennial IAGOD Symposium and Geocongress 2002, 22–26 July 2002, Windhoek, Namibia. Extended Abstracts volume [CD ROM published by the Geological Survey of Namibia].

Frindt, S., Poutiainen, M., 2002. P–T fluid evolution in the Gross Spitzkoppe topaz granite, Namibia. Geological Society of Finland Bulletin 74 (Parts 1–2), 103–114.

Frindt, S., Haapala, I., 2004. Anorogenic Gross Spitzkoppe granite stock in central western Namibia: Part II. Structures and textures indicating crystallization from undercooled melt. American Mineralogist 89, 857–866.

Frindt, S., Haapala, I., Pakkanen, L., 2004a. Anorogenic Gross Spitzkoppe granite stock in central western Namibia. Part I. Petrology and geochemistry. American Mineralogist 89, 841–856.

Frindt, S., Trumbull, R.B., Roemer, R.L., 2004b. Petrogenesis of the Gross Spitzkoppe topaz granite, central western Namibia: a geochemical and Nd–Sr–Pb isotope study. Chemical Geology 206, 43–71.

Frommurze, H.F., Gewers, T.W., Rossouw, P.J., 1942. The geology and mineral deposits of the Karibbib area, South West Africa. Explanation Sheet, vol. 79. Geological Survey of South Africa, Pretoria.

Frost, C.D., Frost, B.R., 1997. Reduced rapakivi-type granites: the tholeiitic connection. Geology 25, 647–650.

Frost, B.R., Barnes, C.G., Collins, W.J., Arculus, R.J., Ellis, D.J., Frost, C.D., 2001. A geochemical classification for granitic rocks. Journal of Petrology 42, 2033–2048.

Garland, F., Hawkesworth, C.J., Mantovani, M.S.M., 1995. Description and petrogenesis of the Paraná rhyolites, southern Brazil. Journal of Petrology 36, 1193–1227.

Gibson, S.A, Thompson, R.N., Dickin, A.P., Leonardos, O.H., 1995. High-Ti and low-Ti mafic potassic magmas: key to plume–lithosphere interactions and continental flood–basalt genesis. Earth and Planetary Science Letters 136, 149–165.

Gladczenko, T.P., Hinz, K., Eldholm, O., Mayer, H., Neben, S., Skogseid, J., 1997. South Atlantic volcanic margins. Journal of the Geological Society of London 154, 465–470.

Haapala, I., 1997. Magmatic and postmagmatic processes in tin-mineralized granites: topaz-bearing leucogranite in the Eurajoki rapakivi granite stock, Finland. Journal of Petrology 38, 1645–1659.

Haapala, I., Rämö, O.T., 1990. Petrogenesis of rapakivi granites of Finland. In: Stein, H.J., Hannah, J.L. (Eds.), Ore-bearing Granitic Systems: Petrogenesis and Mineralizing Processes. Special Paper - Geological Society of America, vol. 246, pp. 275–286.

Haapala, I., Lukkari, S., 2005. Petrological and geochemical evolution of the Kymi stock, a topaz granite cupola within the Wiborg rapakivi granite batholith, Finland. Lithos 80, 347–362.

Haapala, I., Rämö, O.T., Frindt, S., 2005. Comparison of Proterozoic and Phanerozoic rift-related basaltic–granitic magmatism. Lithos 80, 1–32.

Harris, C., 1995. Oxygen isotope geochemistry of the Mesozoic anorogenic complexes of Damaraland, northwest Namibia: evidence of crustal contamination and its effect on silica saturation. Contribution to Mineralogy and Petrology 122, 308–321.

Harris, C., Whittingham, A.M., Milner, S.C., Armstrong, R.A., 1990. Oxygen isotope geochemistry of the silicic rocks of the Etendeka–Paraná Province: source constraints. Geology 18, 1119–1121.

Harris, C., Marsh, J.S., Milner, S.C., 1999. Petrology of the alkaline core of the Messum igneous complex, Namibia: evidence for the progressively decreasing effect of crustal contamination. Journal of Petrology 40, 1377–1397.

Hawkesworth, C., Kelly, S., Turner, le Roex, A., Storey, B., 1999. Mantle processes during Gondwana break-up and dispersal. Journal of African Earth Sciences B 28, 239–261.

Hildreth, W., Halliday, A.N., Christiansen, R.L., 1991. Isotopic and chemical evidence concerning the genesis and contamination of basaltic and rhyolitic magma beneath the Yellowstone Plateau volcanic field. Journal of Geology 32, 63–138.

Huppert, H.F., Sparks, S.J., 1988. The generation of granitic magmas by intrusion of basalt into continental crust. Journal of Petrology 29, 599–624.

Irber, W., 1999. The lanthanide tetrad effect and its correlation with K/Rb, Eu/Eu*, Sr/Eu, Y/Ho, and Zr/Hf of evolving peraluminous granite suites. Geochimica et Cosmochimica Acta 63, 489–508.

Jahn, B., Wu, F., Capdevila, R., Martineau, F., Zhenhua, Z., Wang, Y., 2001. Highly evolved juvenile granites with tetrad REE patterns: the Woduhe and Baerzhe granites from the Great Xing'an Mountains in NE China. Lithos 59, 179–198.

Jung, W., Mezger, K., Hoernes, S., 1998. Petrology and geochemistry of syn- to post-collisional metaluminous A-type granites — major and trace element and Nd–Sr–Pb–O–isotope study from Proterozoic Damars Belt, Namibia. Lithos 45, 147–175.

Jung, S., Hoernes, S., Mezger, K., 2000. Geochronology and petrogenesis of Pan-African, syn-tectonic, S-type and post-tectonic A-type granite (Namibia): products of melting of crustal sources, fractional crystallization and wall rock entrainment. Lithos 50, 268–287.

Jung, S., Mezger, K., Hoernes, S., 2001. Trace element and isotopic (Sr, Nd, Pb, O) arguments for mid-crustal origin of Pan-African garnet-bearing S-type granites from the Damara Orogen (Namibia). Precambrian Research 110, 325–355.

Kandara, J., 1998. Petrography and geochemistry of the Klein Spitzkoppe granite complex, central-western Namibia. Unpublished M.Sc. thesis, Department of Geology, University of Helsinki.

Lenharo, S.L.R., Pollard, P.J., Born, H., 2003. Petrology and textural evolution of granites associated with tin and rare metal mineralization at the Pitinga mine, Amazonas, Brazil. Lithos 66, 37–61.

le Roex, A.P., Lanyon, R., 1998. Isotope and trace element geochemistry of Cretaceous Damaraland lamprophyres and carbonatites, northwestern Namibia: evidence for plume–lithosphere interactions. Journal of Petrology 39, 1117–1146.

Marsh, J.S., Ewart, A., Milner, S.C., Duncan, A.R., Miller, R.McG., 2001. The Etendeka Igneous Province: magma types and their stratigraphic distribution with implications for the evolution of the Paraná–Etendeka flood basalt province. Bulletin of Volcanology 62, 464–486.

Martin, R.F., 2006. A-type granites of crustal origin ultimately result from open-system fenitization-type reactions in an extensional environment. Lithos 91, 125–136.

McDermott, F., Hawkesworth, C.J., 1990. Intracrustal recycling and upper-crustal evolution: a case study from the Pan-African Damara mobile belt, central Namibia. Chemical Geology 83, 263–280.

McDermott, F., Harris, N.B.W., Hawkesworth, C.J., 1996. Geochemical constraints on crustal anatexis: a case study from Pan-African granitoids of Namibia. Contributions to Mineralogy and Petrology 123, 406–423.

McDermott, F., Harris, N.B.W., Hawkesworth, C.J., 2000. Geochemical constraints on the Pan-African granites in the Damara Belt, Namibia. Communications of the Geological Survey of Namibia 12, 139–148.

Milner, S.C., le Roex, A.P., 1996. Isotope characteristics of the Okenyena igneous complex, northwestern Namibia: constraints on the composition of the early Tristan plume and origin of the EM 1 mantle component. Earth and Planetary Science Letters 141, 277–291.

Milner, S.C., le Roex, A.P., O'Connor, J.M., 1995. Age of Mesozoic igneous rocks in northwestern Namibia and their relationship to continental breakup. Journal of the Geological Society of London 152, 97–104.

Mingram, B., Trumbull, R.B., Littman, S., Gerstenberger, H., 2000. A petrogenetic study of anorogenic felsic magmatism in the Cretaceous Paresis ring complex, Namibia: evidence for mixing of crust and mantle-derived components. Lithos 54, 1–22.

Monecke, T., Kempe, U., Monecke, J., Sala, M., Wolf, D., 2002. Tetrad effect in rare earth element distribution patterns: a method of quantification with application to rock and mineral samples from granite-related rare metal deposits. Geochimica et Cosmochimica Acta 66, 1185–1196.

Murphy, D.T., Collers, K.D., Kamber, B.S., 2002. Lamproite from Gaussberg, Antarctica: possible Transition Zone melts of Archaean subducted sediments. Journal of Petrology 43, 981–1001.

Nekvasil, H., Dondolini, A., Horn, J., Filiberto, J., Long, H., Lindsley, D.H., 2004. The origin and evolution of silica-saturated alkalic suites: an experimental study. Journal of Petrology 45, 693–721.

O'Connor, J.M., Duncan, R.A., 1990. Evolution of the Walvis Ridge–Rio Grande Rise hot spot system: implications for African and South American plate motions over plumes. Journal of Geophysical Research 95, 17475–17502.

Pearce, J.A., Harris, N.B.W., Tindle, A.G., 1984. Trace element discrimination diagrams for the tectonic interpretation of granitic rocks. Journal of Petrology 25, 956–983.

Peate, D.W., Hawkesworth, C.J., 1996. Lithospheric to asthenospheric transition in low-Ti flood basalts from southern Paraná, Brazil. Chemical Geology 127, 1–24.

Peccarillo, A., Barberio, M.R., Yirgu, G., Ayalew, D., Barbieri, M., Wu, T.W., 2003. Relationships between mafic and peralkaline silicic magmatism in continental rift settings: a petrological, geochemical and isotopic study of the Gedmesa volcano, Central Ethiopian Rift. Journal of Petrology 44, 2003–2332.

Pirajno, F., 1990. Geology, geochemistry and mineralization of the Erongo volcanic complex, Namibia. South African Journal of Geology 93, 485–504.

Plank, T., Langmuir, C.H., 1998. The chemical composition of subducting sediments and its consequences for the crust and mantle. Chemical Geology 145, 325–394.

Ramdohr, P., 1941. Eine Fundstelle von Beryllium–Mineralien im Gebiet der kleinen Spitzkoppe, Südwestafrika und ihre Paragenesis. Neues Jahrbuch für Mineralogi 76 (Abt. A), 1–35.

Renne, P.R., Glen, J.M., Milner, S.C., Duncan, A.R., 1996. Age of Etendeka flood volcanism and associated intrusions in southwestern Africa. Geology 24, 659–882.

Schmitt, A.K., Emmermann, R., Trumbull, R.B., Bühn, B., Henjes-Kunst, F., 2000. Petrogenesis and $^{40}Ar/^{39}Ar$ geochronology of the Brandberg Complex, Namibia: evidence for a major mantle contribution in metaluminous and peralkaline granites. Journal of Petrology 51, 1207–1239.

Seth, B., Kröner, A., Metzger, K., Nemchin, A., Pidgeon, R.T., Okrusch, M., 1998. Archean to Neoproterozoic magmatic events in the Kaoko belt of NW Namibia and their geodynamic significance. Precambrian Research 92, 341–363.

Štemprok, M., Šulcek, Z., 1969. Geochemical profile through an ore bearing lithium granite. Economic Geology 64, 392–404.

Taylor, R.P., 1992. Petrological and geochemical characteristics of the Pleasant Ridge zinnwaldite–topaz granite, southern New Brunswick, and comparison with other topaz-bearing felsic rocks. Canadian Mineralogist 30, 821–895.

Taylor, R.P., Fallic, A.E., 1997. The evolution of fluorine-rich felsic magmas: source, dichotomy, magmatic convergence and the origins of topaz granite. Terra Nova 9, 105–108.

Thompson, R.N., Gibson, S.A., Dickin, A.P., Smith, P.M., 2001. Early Cretaceous basalt and picrite dykes of the southern Etendeka region, NW Namibia: windows into the role of Tristan mantle plume in the Paraná–Etendeka magmatism. Journal of Petrology 42, 2049–2081.

Trumbull, R.B., Emmermann, R., Bühm, B., Gerstenberger, H., Mingram, B., Schmitt, A., Volker, F., 2000. Insights on the genesis of the Cretaceous Damaraland igneous complexes in Namibia from a Nd- and Sr-isotopic perspective. Communications of the Geological Survey of Namibia 12, 313–324.

Trumbull, R.B., Bühn, B., Romer, R.L., Volker, F., 2003. The petrology of the basanite–tephrite intrusions in the Erongo complex and its implications for a plume origin of Cretaceous alkaline complexes in Namibia. Journal of Petrology 44, 93–112.

Trumbull, R.B., Harris, C., Frindt, S., Wigand, M., 2004. Oxygen and neodymium isotope evidence for source diversity in Cretaceous anorogenic granites from Namibia and implications for A-type granite genesis. Lithos 73, 21–40.

Watson, E.B., Harrison, T.M., 1983. Zircon saturation revisited: temperature and composition effects in a variety of crustal magma types. Earth and Planetary Science Letters 64, 295–304.

Whalen, J.W., Currie, K.L., Chappell, B.W., 1987. A-type granites: geochemical characteristics, discrimination and petrogenesis. Contributions to Mineralogy and Petrology 95, 407–419.

White, R., McKenzie, D., 1989. Magmatism at rift zones: the generation of volcanic continental margins and flood basalts. Journal of Geophysical Research 94, 7685–7729.

Woolley, A.R., 1987. Lithosphere metasomatism and petrogenesis of the Chilwa Province of alkaline igneous rocks and carbonatites, Malawi. Journal of African Earth Sciences 6, 891–898.